Materials Science

AIMS Materials Science, 10(1): 26–39.
DOI: 10.3934/matersci.2023002
Received: 19 August 2022
Revised: 09 October 2022
Accepted: 18 October 2022
Published: 24 November 2022

http://www.aimspress.com/journal/Materials

Research article

Contribution to study the effect of (Reuss, LRVE, Tamura) models on the axial and shear stress of sandwich FGM plate (Ti–6A1–4V/ZrO_2) subjected on linear and nonlinear thermal loads

Rebai Billel*

Faculty of Sciences & Technology, Civil Engineering Department, University of Abbes Laghrour Khenchela, Algeria

* **Correspondence:** Email: billelrebai@yahoo.fr.

Abstract: The principal goal of the current work is to study the impact of three homogenization models (Reuss, LRVE, Tamura) on the axial and shear stress of sandwich functionally graded plate materials subjected on linear and nonlinear thermal loads with static and elastic behavior and it is simply supported using an integral higher shear deformation theory (HSDT). The governing partial differential equations are solved in the spatial coordinate by Navier solution. Those Numerous micromechanical models have been examined to attain the effective material properties of the two-phase FGM plate. The numerical results are compared with those given by other model existing in the literature to confirm the accuracy of the (HSDT). The present results are in good agreement with all models studied of homogenization for all values of the material index and all geometry configurations of the FG-sandwich plates.

Keywords: micromechanics; sandwich FG plate; stress; thermal loads

1. Introduction

Functionally graded materials (FGM) are an advanced composite material class whose vary gradually and continuously in the composition of microstructure constituents through the dimension of the material [1–3]. The behavior composition of FGM reduce the structural weight with increasing its coefficient modulus of stiffness and strength [4–8]. The properties of all constituents can be employed, for example, the toughness of a metal can be mated with the refractoriness of a ceramic, without any compromise in the toughness of the metal side or the refractoriness of the ceramic side [9–14]. The simple rule of mixture (Voigt law) is used to obtain the effective micromechanics material properties in the commencement of research papers. But to assess the effect of the micromechanical models on the structural responses of FG plates several micromechanical models of FGMs have been studied in [14–16]. Gasik has studied different micromechanical models to obtain the effective material properties of FGMs with power-law, Sigmoid, and exponential function distributions of volume fraction across the thickness of the static, buckling, free and forced vibration analyses for simply-supported FG plates resting on an elastic foundation [17]. Akbarzadeh et al. [18] have investigated about the influences of different forms of micromechanical models on FGM pressurized hollow cylinders. They have used the numerical results via finite element method (FEM) analyses for detailed and homogenized models of functionally graded (FG) carbon nanotube reinforced composite (CNTRC) beams. The effect of the imposed temperature field on the response of the FGM plate composed of Metal and Ceramic with the Mori–Tanaka micromechanical method is discussed [19,20].

Shen et al. [21] have studied the small and large amplitude frequency of vibrations are presented for a functionally graded rectangular plate resting on a two-parameter elastic foundation with two kinds of micromechanics models, namely, Voigt model and Mori–Tanaka model. The comparison studies reveal that the difference between these two models is much less compared to the difference caused by different solution methodologies and plate theories. In literature there is no available work treating the impact of the homogenization models on the sandwich FGM plate. In this paper we have studied the impact of (Reuss, LRVE, Tamura) homogenization or micromechanical models on the axial and shear stress of sandwich functionally graded materials plate subjected to linear and nonlinear thermal loads. The static and elastic behavior of the simply supported is considered. Using an integral higher shear deformation theory (HSDT), the governing partial differential equations are solved in the Cartesian coordinate via Navier solution method. Those Numerous micromechanical models have been examined to attain the effective material properties of the two-phase FGM plate (Metal and ceramic). The numerical results are compared with those given by other model existing in the literature to confirm the accuracy of the (HSDT). The present results are in good agreement with all models studied of homogenization for all values of the material index and all geometry configurations of the FG-sandwich plates.

2. Materials and methods

The geometry domain is assumed as a uniform rectangular plate with thickness “h”, length “a”, and width “b” as shown in Figure 1. The plate has three layers. The FG-face sheets are made by two materials metal and ceramic.

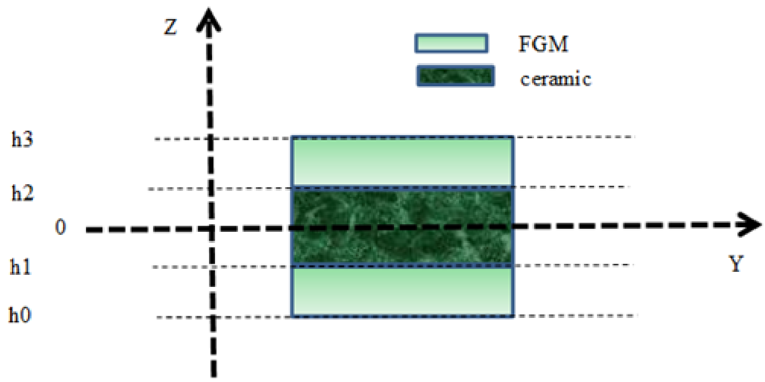

Figure 1. The geometry domain of functionally graded materials plate.

2.1. Materials characteristics

The mechanical and thermal proprieties of Metal (Titanium) are Young modulus $E(z)$ is 66.2 GPa, thermal expansion coefficients α is 10.3 (10^{-6}/K). The mechanical and thermal proprieties of Ceramic (Zirconia) are Young modulus $E(z)$ is 117 GPa, thermal expansion coefficients α is 7.11 (10^{-6}/K). The Poison coefficient is supposed the same in the metal and the ceramic (ν is 1/3). In the following.

Several types of geometries configurations are exanimated depending the thickness of each layer as shown in Table 1.

Table 1. Configurations of the plate.

Configurations of the plate	Geometries with Layers thickness
(1-0-1)	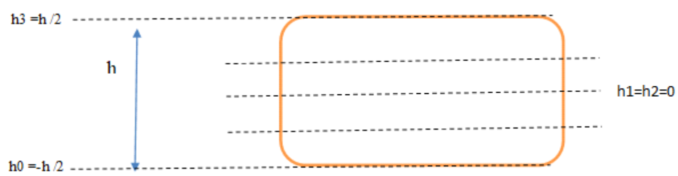
(1-1-1)	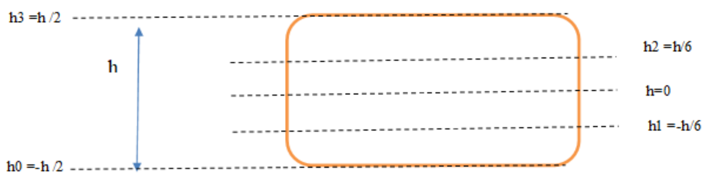
(1-2-1)	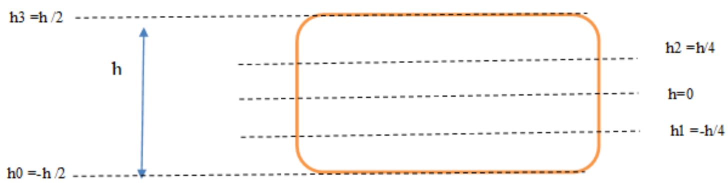

Continued on next page

Configurations of the plate	Geometries with Layers thickness
(2-1-2)	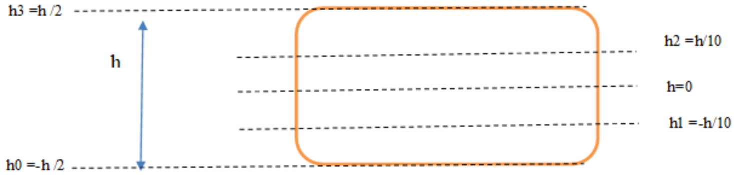
(2-2-1)	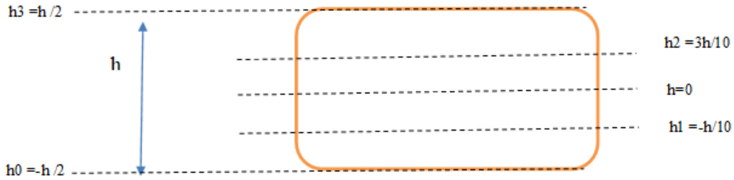

The volumes fraction of the FG- faces sheet are assumed varies as following functions (Eq 1).

$$\begin{aligned} V^{(1)} &= \left(\frac{z-h_0}{h_1 - h_0}\right)^k \qquad z \in [h_0, h_1] \\ V^{(2)} &= 1 \qquad z \in [h_1, h_2] \\ V^{(3)} &= \left(\frac{z-h_3}{h_2 - h_3}\right)^k \qquad z \in [h_2, h_3] \end{aligned} \tag{1}$$

Where K is the material index.

A number of micromechanics models have been proposed for the determination of effective properties of FGMs. K is the material index.

(1) Voigt model

The Voigt model is relatively simple; this model is frequently used in most FGM analyses estimates properties of FGMs as:

$$P(T,z) = P_c(T,z)V(z) + P_m(T,z)(1 - V(z)) \tag{2}$$

(2) Reuss model

Reuss assumed the stress uniformity through the material and obtained the effective properties as:

$$P(T,z) = \frac{P_c(T,z)P_m(T,z)}{P_c(T,z)(1-V(z)) + P_m(T,z)V(z)} \tag{3}$$

(3) Tamura model

The Tamura model uses actually a linear rule of mixtures, introducing one empirical fitting parameter known as “stress-to-strain transfer”. For q = 0 correspond to Reuss rule and with $q = \pm\infty$ to the Voigt rule, being invariant to the consideration of with phase is matrix and which is particulate. The effective property is found as:

$$P(T,z)=\frac{(1-V(z))P_m(T,z)(q-P_c(T,z))+V(z)P_c(T,z)(q-P_m(T,z))}{(1-V(z))(q-P_c(T,z))+V(z)P_c(T,z)(q-P_m(T,z))} \text{ with } q=\frac{\sigma_1-\sigma_2}{\varepsilon_1-\varepsilon_2} \tag{4}$$

(4) Description by a representative volume element (LRVE)

The LRVE is developed based on the assumption that the microstructure of the heterogeneous material is known. The input for the LRVE for the deterministic micromechanical framework is usually volume average or ensemble average of the descriptors of the microstructures.

The effective property is expressed as follows by the LRVE method:

$$P(T,z)=P_m(T,z)\left(1+\frac{V(z)}{\dfrac{1}{1-\dfrac{P_m(T,z)}{P_c(T,z)}}-\sqrt[3]{V(z)}}\right) \tag{5}$$

2.2. Displacement base field

Based on the same assumptions of the conventional HSDT (with fives variables or more). The displacement field of the proposed HSDT is only with four unknowns variables and can be written in a simpler form as:

$$\begin{cases} u(x,y,z)=u_0(x,y)-z\dfrac{\partial w_0}{\partial x}+k_1\, f(z)\displaystyle\int\theta(x,y)\,dx \\ v(x,y,z)=v_0(x,y)-z\dfrac{\partial w_0}{\partial y}+k_2\, f(z)\displaystyle\int\theta(x,y)\,dy \\ w(x,y,z)=w_0(x,y) \end{cases} \tag{6}$$

Where $u_0(x,y)$, $v_0(x,y)$, $w_0(x,y)$, and $\theta(x,y)$ are the four-unknown displacement functions of middle surface of the FG-sandwich plate. $f(z)$ is the warping function and (k_1 and k_2) are constants.

In the current research work the proposed combined (exponential/hyperbolic) warping function ensures the nullity condition of the free surfaces of the FG-sandwich plate (zero transverse shear stresses at top and the Bottom of the FG-sandwich plate). The present exponential/hyperbolic warping function $f(z)$ is expressed as:

$$f(z)=\left[\ln\left(\pi\exp\left(\frac{1}{20}\right)\right)-\left((0.1407)^{(5/6)}\right)\cosh(\pi z)\right]z \tag{7}$$

The stresses/strains linear relation of the PFG-sandwich plate can be expressed as:

$$\begin{Bmatrix}\sigma_x\\ \sigma_y\\ \tau_{xy}\\ \tau_{yz}\\ \tau_{xz}\end{Bmatrix}^{(n)}=\begin{bmatrix}C_{11} & C_{12} & 0 & 0 & 0\\ C_{12} & C_{22} & 0 & 0 & 0\\ 0 & 0 & C_{66} & 0 & 0\\ 0 & 0 & 0 & C_{44} & 0\\ 0 & 0 & 0 & 0 & C_{55}\end{bmatrix}^{(n)}\begin{Bmatrix}\varepsilon_x-\alpha T\\ \varepsilon_y-\alpha T\\ \gamma_{xy}\\ \gamma_{yz}\\ \gamma_{xz}\end{Bmatrix}^{(n)} \tag{8}$$

Where

$$\begin{cases}C_{11}^{(n)}=C_{22}^{(n)}=\dfrac{E^{(n)}(z)}{1-(\nu^{(n)})^2}\\ C_{11}^{(n)}=\nu^{(n)}C_{11}^{(n)}\\ C_{44}^{(n)}=C_{55}^{(n)}=C_{66}^{(n)}=\dfrac{E^{(n)}(z)}{2\left(1+\nu^{(n)}\right)},\end{cases} \tag{9}$$

The variation of the temperature field across the thicness is assumed to be:

$$T(x,y,z)=T_1(x,y)+\frac{z}{h}T_2(x,y)+\frac{\Psi(z)}{h}T_3(x,y) \tag{10}$$

Where

$$\Psi(z)=\frac{h}{\pi}\sin\left(\frac{\pi z}{h}\right) \tag{11}$$

The principle of virtual works of the considered PFG-sandwich plates is expressed as $\delta U+\delta V=0$ where δU is the variation of strain energy; and δV is the variation of the virtual work done by external load applied to the plate. The governing equations can be obtained as follows:

$$\begin{cases}\delta u_0: & \dfrac{\partial N_x}{\partial x}+\dfrac{\partial N_{xy}}{\partial y}=0\\ \delta v_0: & \dfrac{\partial N_{xy}}{\partial x}+\dfrac{\partial N_y}{\partial y}=0\\ \delta w_0: & \dfrac{\partial^2 M_x^b}{\partial x^2}+2\dfrac{\partial^2 M_{xy}^b}{\partial x\partial y}+\dfrac{\partial^2 M_y^b}{\partial y^2}=0\\ \delta\theta: & -\mathrm{k}_1 M_x^s-\mathrm{k}_2 M_y^s-\left(k_1A'+k_2B'\right)\dfrac{\partial^2 M_{xy}^s}{\partial x\partial y}+k_1A'\dfrac{\partial S_{xz}^s}{\partial x}+k_2B'\dfrac{\partial S_{yz}^s}{\partial y}=0\end{cases} \tag{12}$$

Based on the Navier method, the following expansions of displacements are

$$\begin{Bmatrix} u_0 \\ v_0 \\ w_0 \\ \theta \end{Bmatrix} = \begin{Bmatrix} U\cos(\alpha\, x)\sin(\beta\, y) \\ V\sin(\alpha\, x)\cos(\beta\, y) \\ W\sin(\alpha\, x)\sin(\beta\, y) \\ X\sin(\alpha\, x)\sin(\beta\, y) \end{Bmatrix} \tag{13}$$

where (U, V, W, X) are unknown functions to be determined and $\alpha = \pi / a$ and $\beta = \pi / b$.

In the present work, the transverse temperature loads T1, T2, and T3 in double sinus series form as:

$$\begin{Bmatrix} T_1 \\ T_2 \\ T_3 \end{Bmatrix} = \begin{Bmatrix} \overline{T}_1 \\ \overline{T}_2 \\ \overline{T}_3 \end{Bmatrix} \sin(\alpha\, x)\sin(\beta\, y) \tag{14}$$

The closed-form solution can be written as following matrix form:

$$\begin{bmatrix} S_{11} & S_{12} & S_{13} & S_{14} \\ S_{12} & S_{22} & S_{23} & S_{24} \\ S_{13} & S_{23} & S_{33} & S_{34} \\ S_{14} & S_{24} & S_{34} & S_{44} \end{bmatrix} \begin{Bmatrix} U \\ V \\ W \\ X \end{Bmatrix} = \begin{Bmatrix} P_1 \\ P_2 \\ P_3 \\ P_4 \end{Bmatrix} \tag{15}$$

Where

$$\begin{cases} S_{11} = -\left(A_{11}\alpha^2 + A_{66}\beta^2\right) \\ S_{12} = -\alpha\beta\left(A_{12} + A_{66}\right) \\ S_{13} = \alpha\left(B_{11}\alpha^2 + B_{12}\beta^2 + 2B_{66}\beta^2\right) \\ S_{14} = \alpha\left(k_1 B_{11}^s + k_2 B_{12}^s - \left(k_1 A' + k_2 B'\right) B_{66}^s \beta^2\right) \\ S_{22} = -\left(A_{66}\alpha^2 + A_{22}\beta^2\right) \\ S_{23} = \beta\left(B_{22}\beta^2 + B_{12}\alpha^2 + 2B_{66}\alpha^2\right) \\ S_{24} = \beta\left(k_2 B_{22}^s + k_1 B_{12}^s - \left(k_1 A' + k_2 B'\right) B_{66}^s \alpha^2\right) \\ S_{33} = -\left(D_{11}\alpha^4 + 2(D_{12} + 2D_{66})\alpha^2\beta^2 + D_{22}\beta^4\right) \\ S_{34} = -k_1\left(D_{11}^s\alpha^2 + D_{12}^s\beta^2\right) + 2(k_1 A' + k_2 B') D_{66}^s \alpha^2\beta^2 - k_2\left(D_{22}^s\beta^2 + D_{12}^s\alpha^2\right) \\ S_{44} = -k_1\left(H_{11}^s k_1 + H_{12}^s k_2\right) - (k_1 A' + k_2 B')^2 H_{66}^s \alpha^2\beta^2 - k_2\left(H_{12}^s k_1 + H_{22}^s k_2\right) - \left(k_1 A'\right)^2 A_{55}^s \alpha^2 - \left(k_2 B'\right)^2 A_{44}^s \beta^2 \end{cases} \tag{16}$$

And

$$\begin{cases} P_1 = \alpha(A^T T_1 + B^T T_2 + {}^aB^T T_3) \\ P_2 = \beta(A^T T_1 + B^T T_2 + {}^aB^T T_3) \\ P_3 = -h(\alpha^2 + \beta^2)(B^T T_1 + D^T T_2 + {}^aD^T T_3) \\ P_4 = -h(\alpha^2 + \beta^2)({}^sB^T T_1 + {}^sD^T T_2 + {}^sF^T T_3) \end{cases} \tag{17}$$

Where and $(L^T, {}^aL^T, R^T)$ are coefficients calculated by integral summation formulations, in which $\overline{z} = z / h, \overline{f}(z) = f(z) / h$ and $\overline{\psi}(z) = \psi(z) / h$.

3. Results and discussion

In the following three sections, the results have been presented.

3.1. Comparisons and validation

A comparison has been done to verify the accuracy of the present theory of different models of homogenization (Reuss, Tamura and LRVE). Results are compared with the mixture model (Voigt) using by Zankour and Algamidi [22].

The dimensionless transverse and normal stress are expressed as:

$$\begin{cases} \bar{\sigma}_x = \dfrac{h^2}{\alpha_0 \bar{T}_2 E_0 a^2} \sigma_x\left(\dfrac{a}{2}, \dfrac{b}{2}, \dfrac{h}{2}\right) \\ \bar{\tau}_{xz} = \dfrac{10h}{\alpha_0 \bar{T}_2 E_0 a} \tau_{xz}\left(0, \dfrac{b}{2}, 0\right) \end{cases} \tag{18}$$

with $E_0 = 1GPa$ and $\alpha_0 = 10^6\,K$.

Table 2. Axial stresses $\bar{\sigma}_x$ of the FG square plates (T3 = 0).

k	Theory		$\bar{\sigma}_x$				
			1-0-1	1-1-1	1-2-1	2-1-2	2-2-1
0	Zankour	Voigt	−2.079675000	−2.079675000	−2.079675000	−2.079675000	−2.079675000
	Present	Reuss	−2.079675000	−2.079675000	−2.079675000	−2.079675000	−2.079675000
		LRVE	−2.079675000	−2.079675000	−2.079675000	−2.079675000	−2.079675000
		Tamura	−2.079675000	−2.079675000	−2.079675000	−2.079675000	−2.079675000
1	Zenkour	Voigt	−1.993962994	−2.144483622	−2.262070783	−2.071720141	−2.276270538
	Present	Reuss	−2.054001279	−2.206426851	−2.319985581	−2.133961897	−2.328859434
		LRVE	−2.019721781	−2.170723580	−2.286705796	−2.098127768	−2.298783479
		Tamura	−2.054001279	−2.206426851	−2.319985581	−2.133961897	−2.328859434
3	Zenkour	Voigt	−1.764722947	−1.912070024	−2.065545648	−1.830280890	−2.099358095
	Present	Reuss	−1.780352582	−1.937106476	−2.093543390	−1.851668884	−2.122979641
		LRVE	−1.772412913	−1.923584710	−2.078438949	−1.840257943	−2.110349605
		Tamura	−1.780352582	−1.937106476	−2.093543390	−1.851668884	−2.122979641
5	Zenkour	Voigt	−1.726018586	−1.851951252	−2.008943548	−1.775782946	−2.052753400
	Present	Reuss	−1.731998461	−1.865654772	−2.025948107	−1.786255940	−2.066835810
		LRVE	−1.729130531	−1.858346729	−2.016889735	−1.780777417	−2.059428200
		Tamura	−1.731998461	−1.865654772	−2.025948107	−1.786255940	−2.066835810

Table 2 presents the variation of dimensionless axial stress "$\bar{\sigma}_x$" of the square FG-sandwich plate subjected to linearly thermal load "$T_3 = 0$" versus volumes fractions (material index "k") for different values of layer thickness ratio. It is remarkable that there is a proportional relationship between the index "k" the dimensionless normal stress "$\bar{\sigma}_x$".

Table 3. Shear stresses $\bar{\tau}_{xz}$ of the FGM square plates (T3 =−100).

k	Theory		$\bar{\tau}_{xz}$				
			1-0-1	1-1-1	1-2-1	2-1-2	2-2-1
0	Zenkour	Voigt	0.4146850492	0.4146850448	0.4146850391	0.4146850437	0.4146850439
	Present	Reuss	0.4146850492	0.4146850448	0.4146850391	0.4146850437	0.4146850439
		LRVE	0.4146850492	0.4146850448	0.4146850391	0.4146850437	0.4146850439
		Tamura	0.4146850492	0.4146850448	0.4146850391	0.4146850437	0.4146850439
1	Zenkour	Voigt	0.5088666494	0.5057769569	0.5120235930	0.5028076163	0.5078946003
	Present	Reuss	0.5136021296	0.4984428129	0.4996166330	0.4989271190	0.4972491537
		LRVE	0.5087063178	0.5006052702	0.5045310781	0.4991788650	0.4946850439
		Tamura	0.5136021296	0.4984428129	0.4996166330	0.4989271190	0.4972491537
3	Zenkour	Voigt	0.5103204312	0.5033093833	0.5165886526	0.4976909215	0.5100386919
	Present	Reuss	0.5238780098	0.5054862362	0.5169250930	0.5015862328	0.5102636411
		LRVE	0.5156350522	0.5037663327	0.5159615534	0.4988965994	0.5012769094
		Tamura	0.5238780098	0.5054862362	0.5169250930	0.5015862328	0.5102636411
5	Zenkour	Voigt	0.5212843911	0.4908722755	0.5036863726	0.4852538506	0.5661515630
	Present	Reuss	0.5357072550	0.4919895199	0.5166537262	0.4878864038	0.5084226158
		LRVE	0.5281264494	0.4913047274	0.5153580228	0.4862334163	0.5071304901
		Tamura	0.5357072550	0.4919895199	0.5166537262	0.4878864038	0.5084226158

The Table 3 presents the variation of the dimensionless shear stress "$\bar{\tau}_{xz}$" of the square FG-sandwich plate subjected to nonlinearly thermal load "$T_3 = -100$" versus volumes fractions (material index "k") for different values of layer thickness ratio .from the Table 3 the shear stress "$\bar{\tau}_{xz}$" and the index k have direct relation. We can see from the Tables 2 and 3 that the present results are in good agreement with all models studied of homogenization (Voigt Zenkour et al. [22], Reuss, LRVE and Tamura) for all values of the material index "k" and all configurations of the FG-sandwich plate (1-0-1, 1-1-1, 1-2-1, 2-1-2 and 2-2-1).

3.2. Parametric study

In this section, the parametric studies are presented in the explicit graphs form. Figure 2 plots the variation of the axial stress "$\bar{\sigma}_x$" across the total thickness "h" of FG-sandwich plate ($k = 1$) under linear thermal loads "$T_3 = 0$" with different micromechanical models. From the plotted graphs, it is clear that the compressive stresses are obtained at the top of the plate. We can see that the present results are in good agreement with different models Voigt, Reuss, LRVE and Tamura for configurations of the FG-sandwich plate (1-0-1, 1-2-1 and 2-2-1) and the material index $k = 1$ (Figure 2a–c).

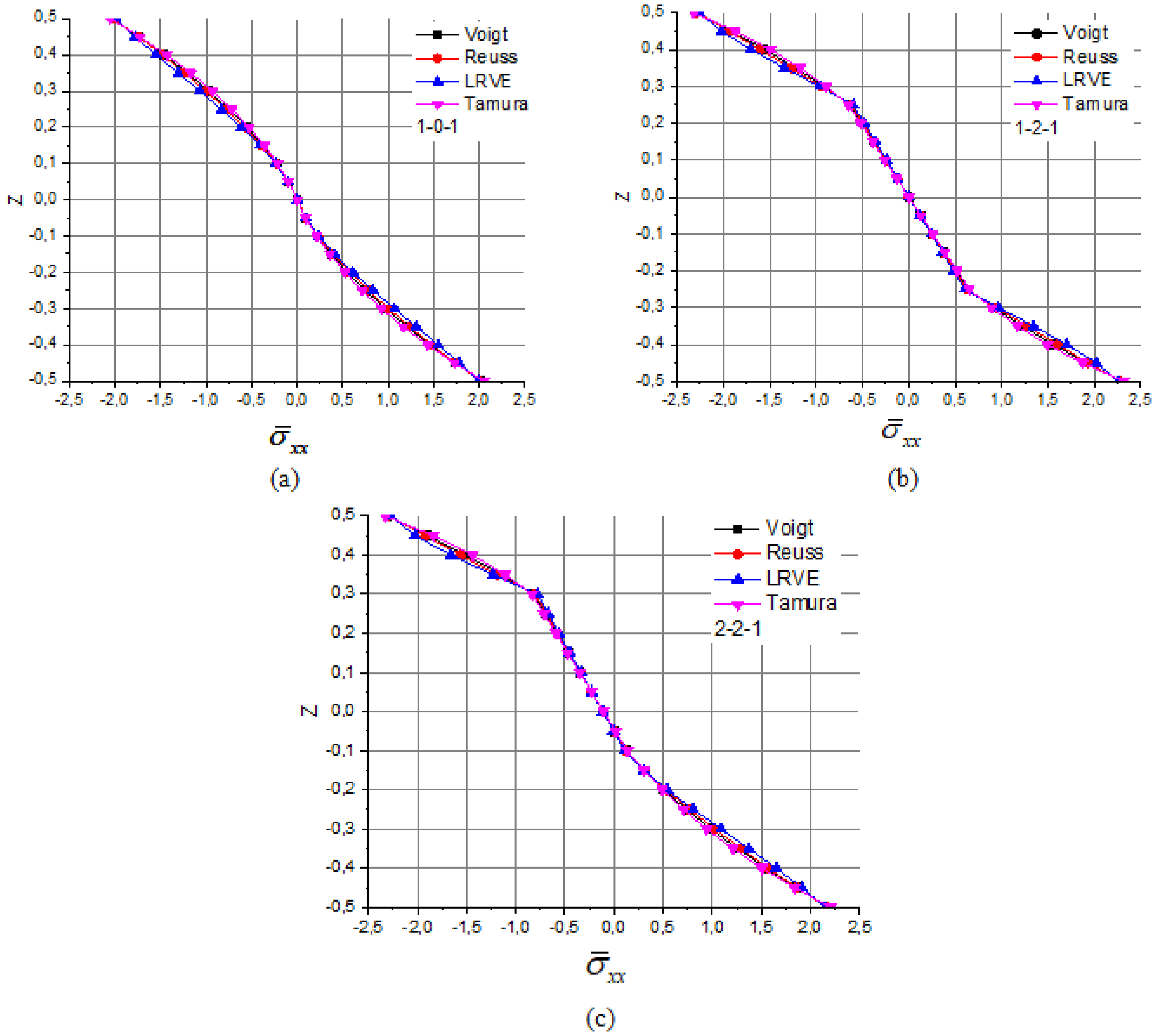

Figure 2. Effect of different micromechanical models on the axial stress $\bar{\sigma}_{xx}$ of FG-sandwich.

Figure 3 illustrates the variation of the "$\bar{\tau}_{xz}$" through the total thickness of the 1-0-1, 1-2-1 and 2-2-1 FG-sandwich plate under linear thermal loads "$T_3 = 0$". It is noted that the shear stress "$\bar{\tau}_{xz}$" is parabolically varied through the total thickness of the FG-sandwich plate. We can see that the present results are in good agreement with different models Voigt, Reuss, LRVE and Tamura for configurations of the FG-sandwich plate (1-0-1, 1-2-1 and 2-2-1) and the material index $k = 1$ (Figure 3a–c).

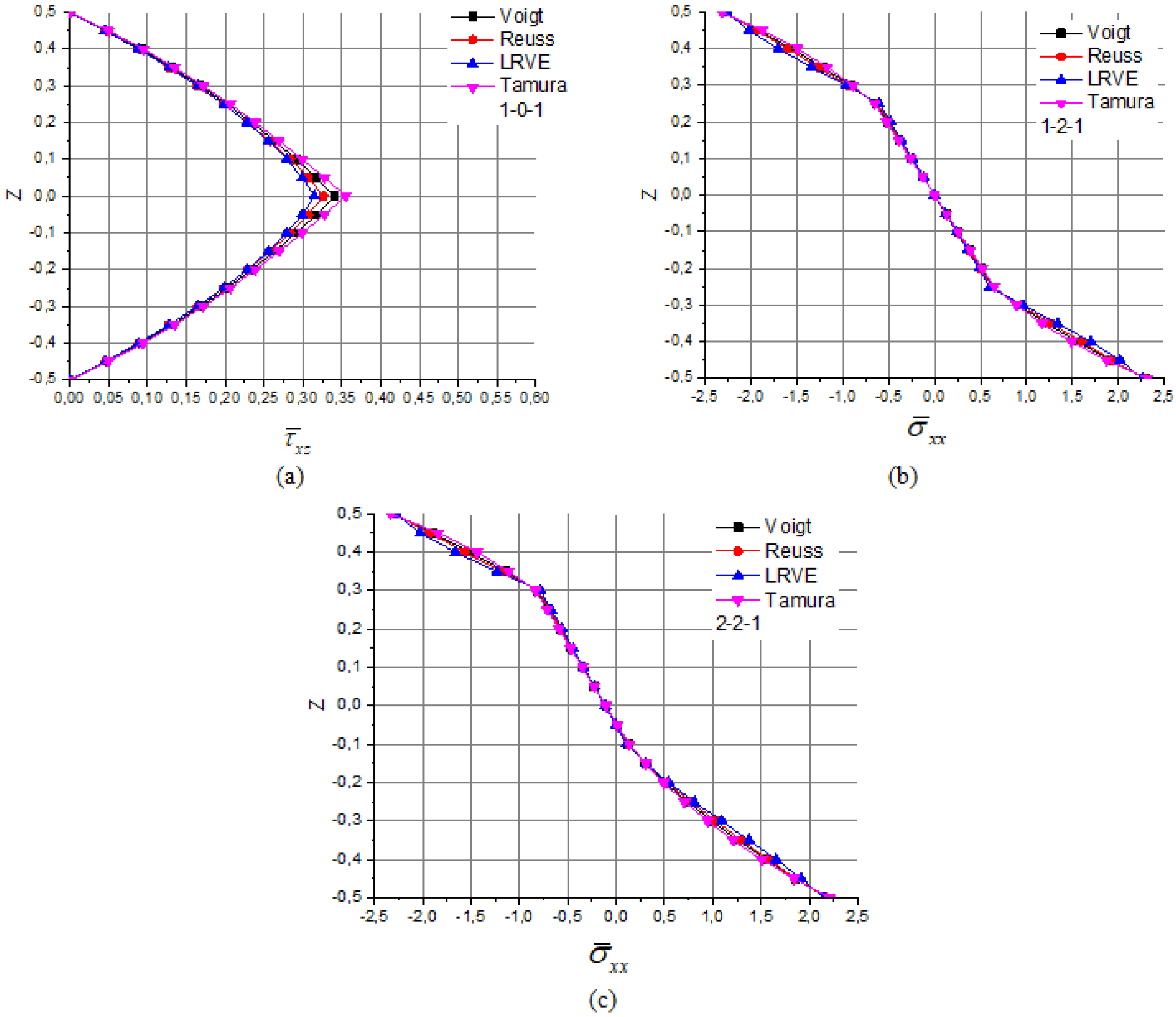

Figure 3. Effect of different micromechanical models on the axial stress $\bar{\sigma}_{xx}$ of FG-sandwich.

3.3. *Effect of the thermal loads on the normal and shear stress*

In the present section three types of the temperature distribution across the thickness are considered. The first one, the temperature is linearly distributed through the thickness $T = zT_2$, in the second type the temperatures vary nonlinearly across h ($T = zT_2 + \psi(z)T_3$) and the third type is reserved for a combination of linear and nonlinear distributions $T(z) = T_1 + (z/h)T_2 + (\Psi(z)/h)T_3$.

Figure 4a shows the distributions of the axial stress "$\bar{\sigma}_x$" through the total thickness of the simply supported 2-2-1 FG-sandwich plate for various values of the thermal load ($T_1 = 100$), $T_2 = 100$ and $T_3 = 100$ with ($k = 1$). From the plotted curves, it can be observed that the axial stress "$\bar{\sigma}_x$" is c influenced by the values of the thermal load.

Figure 4b plot the variation of the shear stress "$\bar{\tau}_{xz}$" through the thickness h of the 2-2-1 square FG-sandwich plate ($k = 1$). For different values of the thermal load ($T_1 = 100$), $T_2 = 100$ and $T_3 = 100$. It can be noted from the graphs that the shear stress "$\bar{\tau}_{xz}$" has a parabolic variation through the thickness. The maximal values of the shear stress "$\bar{\tau}_{xz}$" are obtained at the mid-plane axis "$\bar{z} = 0$". And it is clearly influenced by the values of the thermal load.

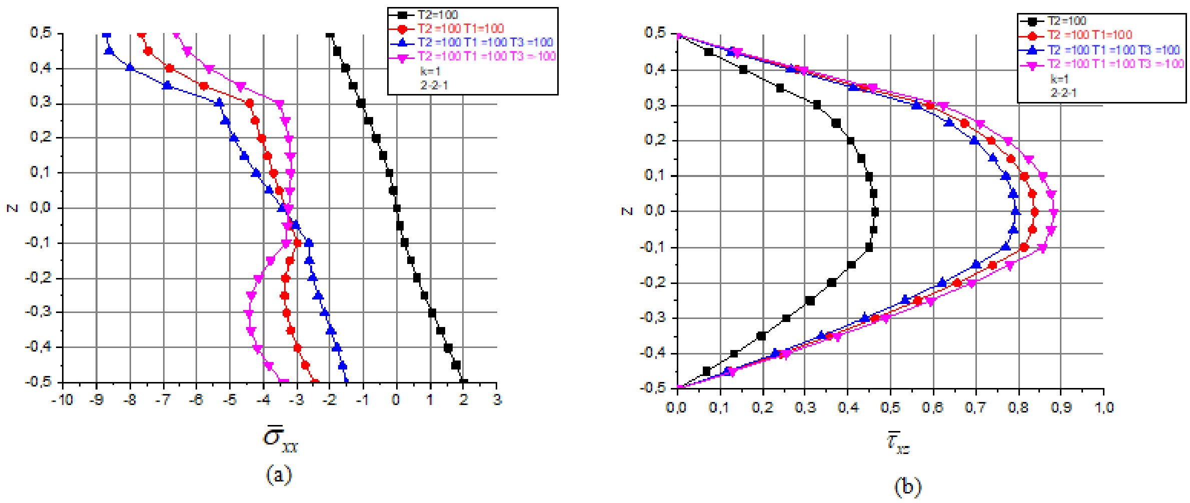

Figure 4. Effect of the thermal load T1, T2 and T3 on the axial and transvers stress ($\bar{\sigma}_{xx}$, $\bar{\tau}_{xz}$) of the (2-2-1) FG-sandwich plate (k = 1) for Voigt model.

4. Conclusions

In this investigation, the impact of (Reuss, LRVE, Tamura) homogenization or micromechanical models on the axial and shear stress of sandwich functionally graded materials plate subjected to linear and nonlinear thermal loads have studied. The static and elastic behavior of the simply supported is considered. Using an integral higher shear deformation theory (HSDT), the governing partial differential equations are solved in the Cartesian coordinate via Navier solution method. Those Numerous micromechanical models have been examined to attain the effective material properties of the two-phase FGM plate (Metal and ceramic). The numerical results are compared with those given by other model existing in the literature to confirm the accuracy of the (HSDT). The present results are in good agreement with all models studied of homogenization for all values of the material index and all geometry configurations of the FG-sandwich plates.

Acknowledgments

The authors gratefully acknowledge the support provided by University of Sidi Bel Abbes, Algeria while the preparation of the doctorate thesis.

Conflict of interest

The authors declare no conflict of interest.

References

1. Venâncio MAS, Loja A (2016) A study on the behavior of laminated and sandwich composite plates using a layerwise theory. *AIMS Mater Sci* 3: 1587–1614. https://doi.org/10.3934/matersci.2016.4.1587
2. Salleh Z, Islam MM, Epaarachchi JA, et al. (2016) Mechanical properties of sandwich composite made of syntactic foam core and GFRP skins. *AIMS Mater Sci* 3: 1704–1727. https://doi.org/10.3934/matersci.2016.4.1704
3. Abood AM, Khazal H, Hassan AF (2022) On the determination of first-mode stress intensity factors and T-stress in a continuous functionally graded beam using digital image correlation method. *AIMS Mater Sci* 9: 56–70. https://doi.org/10.3934/matersci.2022004
4. Bash AM, Mnawe SE, Salah SA (2020) Numerical buckling analysis of carbon fibre-epoxy composite plates with different cutouts number by finite element method. *AIMS Mater Sci* 7: 46–59. https://doi.org/10.3934/matersci.2020.1.46
5. Sánchez CA, Cardona-Maya Y, Morales AD, et al. (2021) Development and evaluation of polyvinyl alcohol films reinforced with carbon nanotubes and alumina for manufacturing hybrid metal matrix composites by the sandwich technique. *AIMS Mater Sci* 8: 149–165. https://doi.org/10.3934/matersci.2021011
6. Saberi S, Abdollahi A, Inam F (2021) Reliability analysis of bistable composite laminates. *AIMS Mater Sci* 8: 29–41. https://doi.org/10.3934/matersci.2021003
7. Ishchuk V, Kuzenko D, Sobolev V (2018) Piezoelectric and functional properties of materials with coexisting ferroelectric and antiferroelectric phases. *AIMS Mater Sci* 5: 711–741. https://doi.org/10.3934/matersci.2018.4.711
8. Kozhakhmetov Y, Skakov M, Wieleba W, et al. (2020) Evolution of intermetallic compounds in Ti-Al-Nb system by the action of mechanoactivation and spark plasma sintering. *AIMS Mater Sci* 7: 182–191.
9. Costa S, Souza MS, Braz-César MT, et al. (2021) Experimental and numerical study to minimize the residual stresses in welding of 6082-T6 aluminum alloy. *AIMS Mater Sci* 8: 271–282. https://doi.org/10.3934/matersci.2021018
10. Abdellah MY, Alharthi H, Hassan MK, et al. (2020) Effect of specimen size on natural vibration of open hole copper/glass-reinforced epoxy laminate composites. *AIMS Mater Sci* 7: 499–517. https://doi.org/10.3934/matersci.2020.4.499
11. Soyama H, Okura Y (2018) The use of various peening methods to improve the fatigue strength of titanium alloy Ti6Al4V manufactured by electron beam melting. *AIMS Mater Sci* 5: 1000-1015. https://doi.org/10.3934/matersci.2018.5.1000
12. Esquivel Merino MD, Van Der Voort P, Romero-Salguero F (2014) Designing advanced functional periodic mesoporous organosilicas for biomedical applications. *AIMS Mater Sci* 1: 70–86. https://doi.org/10.3934/matersci.2014.1.70
13. Nie G, Zhong Z (2010) Dynamic analysis of multi-directional functionally graded annular plates. *Appl Math Model* 34: 608–616. https://doi.org/10.1016/j.apm.2009.06.009
14. Tucker III, Charles L, Liang E (1999) Stiffness predictions for unidirectional short-fiber composites: Review and evaluation. *Compos Sci Technol* 59: 655–671. https://doi.org/10.1016/S0266-3538(98)00120-1

15. Kim JH, Paulino GH (2003) An accurate scheme for mixed-mode fracture analysis of functionally graded materials using the interaction integral and micromechanics models. *Int J Numer Meth Eng* 58: 1457–1497. https://doi.org/10.1002/nme.819
16. Zuiker JR (1995) Functionally graded materials: Choice of micromechanics model and limitations in property variation. *Comp Eng* 5: 807–819. https://doi.org/10.1016/0961-9526(95)00031-H
17. Gasik MM (1998) Micromechanical modelling of functionally graded materials. *Comp Mater Sci* 13: 42-55. https://doi.org/10.1016/S0927-0256(98)00044-5
18. Akbarzadeh AH, Abedini A, Chen ZT (2015) Effect of micromechanical models on structural responses of functionally graded plates. *Compos Struct* 119: 598-609. https://doi.org/10.1016/j.compstruct.2014.09.031
19. Praveen GN, Reddy JN (1998) Nonlinear transient thermoelastic analysis of functionally graded ceramic-metal plates. *Int J Solids Struct* 35: 4457–4476. https://doi.org/10.1016/S0020-7683(97)00253-9
20. Jin X, Wu LZ, Guo LC, et al. (2009) Prediction of the variation of elastic modulus in ZrO_2/NiCr functionally graded materials. *Compos Sci Technol* 69: 1587–1591. https://doi.org/10.1016/j.compscitech.2009.02.032
21. Shen HS, Wang ZX (2012) Assessment of voigt and Mori-Tanaka models for vibration analysis of functionally graded plates. *Compos Struct* 94: 2197–2208. https://doi.org/10.1016/j.compstruct.2012.02.018
22. Zenkour AM, Alghamdi NA (2008) Thermoelastic bending analysis of functionally graded sandwich plates. *J Mater Sci* 43: 2574–2589. https://doi.org/10.1007/s10853-008-2476-6